Clinical and Translational Radiation Oncology 46 (2024) 100772

Contents lists available at ScienceDirect

Clinical and Translational Radiation Oncology

journal homepage: www.sciencedirect.com/journal/clinical-and-translational-radiation-oncology

High-dose loco-regional pattern of failure after primary radiotherapy in p16 positive and negative head and neck squamous cell carcinoma – A DAHANCA 19 study

Morten Horsholt Kristensen [a,*], Anne Ivalu Sander Holm [b], Christian Rønn Hansen [c,d,e], Ruta Zukauskaite [f], Eva Samsøe [g], Christian Maare [h], Jørgen Johansen [f], Hanne Primdahl [b], Åse Bratland [i], Claus Andrup Kristensen [j], Maria Andersen [k], Jens Overgaard [a], Jesper Grau Eriksen [a]

[a] Department of Experimental Clinical Oncology, Aarhus University Hospital, Palle Juul-Jensens Boulevard 99, 8200 Aarhus N, Denmark
[b] Department of Oncology, Aarhus University Hospital, Palle Juul-Jensens Boulevard 99, 8200 Aarhus N, Denmark
[c] Laboratory of Radiation Physics, Odense University Hospital, Sdr. Boulevard 29, 5000 Odense C, Denmark
[d] Danish Centre for Particle Therapy, Aarhus University Hospital, Palle Juul-Jensens Boulevard 25, 8200 Aarhus N, Denmark
[e] Department of Clinical Research, University of Southern Denmark, Sdr. Boulevard 29, 5000 Odense C, Denmark
[f] Department of Oncology, Odense University Hospital, Sdr. Boulevard 29, 5000 Odense C, Denmark
[g] Department of Oncology, Zealand University Hospital, Rådmandsengen 5, 4700 Næstved, Denmark
[h] Department of Oncology, Copenhagen University Hospital – Herlev, Borgmester Ib Juuls Vej 1, 2730 Herlev, Denmark
[i] Department of Oncology, Oslo University Hospital, Ullernchausseen 70, 0372 Oslo, Norway
[j] Department of Oncology, Copenhagen University Hospital – Rigshospitalet, Blegdamsvej 9, 2100 Copenhagen, Denmark
[k] Department of Oncology, Aalborg University Hospital, Hobrovej 18, 9000 Aalborg, Denmark

ARTICLE INFO

Keywords:
Radiotherapy (RT)
Head and neck squamous cell carcinoma (HNSCC)
Pattern of failure
Human papilloma virus (HPV)/p16
Radiobiology
Radioresistance
Deformable image registration (DIR)
Point of origin

ABSTRACT

Introduction: Patients with failure after primary radiotherapy (RT) for head and neck squamous cell carcinoma (HNSCC) have a poor prognosis. This study investigates pattern of failure after primary curatively intended IMRT in a randomized controlled trial in relation to HPV/p16 status.
Material and methods: Patients with HNSCC of the oral cavity, oropharynx (OPSCC), hypopharynx or larynx were treated with primary curative IMRT (+/-cisplatin) and concomitant nimorazole between 2007 and 12. Of 608 patients, 151 had loco-regional failure within five years, from whom 130 pairs of scans (planning-CT and diagnostic failure scan) were collected and deformably co-registered. Point of origin-based pattern of failure analysis was conducted, including distance to CTV1 and GTV, and estimated dose coverage of the point of origin.
Results: Of 130 patients with pairs of scans, 104 (80 %) had at least one local or regional failure site covered by 95 % of prescribed dose and 87 (67 %) of the failures had point of origin within the high-dose CTV (CTV1). Of failures from primary p16 + OPSCC, the majority of both mucosal (84 %) and nodal (61 %) failures were covered by curative doses. For p16− tumors (oral cavity, OPSCC p16neg, hypopharynx and larynx), 75 % of mucosal and 66 % of nodal failures were high-dose failures.
Conclusion: Radioresistance is the primary cause of failure after RT for HNSCC irrespective of HPV/p16 status. Thus, focus on predictors for the response to RT is warranted to identify patients with higher risk of high-dose failure that might benefit from intensified treatment regimens.

Introduction

The ultimate goal of curatively intended radiotherapy (RT) for head and neck squamous cell carcinoma (HNSCC) is to obtain loco-regional control. When failure occurs subsequent to treatment, the prognosis for the patient is poor, with only one out of four patients achieving lasting tumor control after treatment for the failure [1]. When treatment fails loco-regionally after primary curative RT, two scenarios may be

* Corresponding author.
E-mail address: mortenhorsholt@oncology.au.dk (M.H. Kristensen).

https://doi.org/10.1016/j.ctro.2024.100772
Received 7 December 2023; Received in revised form 28 February 2024; Accepted 29 March 2024
Available online 30 March 2024

envisaged, either the failure was due to lack of RT dose coverage (geographical miss) or failure occurred despite coverage by high-dose radiation. In the latter case, the cause of failure might be explained by biological factors, including high density of cancer stem cells (CSC) [2,3] or correlated to the effects of HPV. Thus, HPV-driven cell lines of head and neck cancer have been shown to have a more radiosensitive profile than HPV-negative cell lines [4,5]. However, the prognostic value of p16 is limited to oropharyngeal tumors [6].

When loco-regional failure occurs after curative RT, the failure most often originates in relation to the primary high-dose region [7–19]; regardless of the method applied to characterize failures in relation to the original RT plan, most failures were related to high-dose targets. Either the largest proportion of failures had a significant overlap with high-dose target volumes/high-dose 95 % isodose [7–12,14,15,17,18] (volumetric approach) or as having a point of origin (PO) inside high-dose volume/covered by 95 % of prescribed dose [7,9,11,13,16,20]. Few patterns of failure studies have stratified for HPV-status, and only with volumetric-based analysis [8,10,21,22]. These four studies have diverged results on the pattern of failure in patients with primary HPV-driven oropharyngeal squamous cell carcinoma (OPSCC).

With the overall aim of identifying tumors where the failure was located in the high-dose volume (high-dose failures), this study investigated the PO-based pattern of failure in relation to high-dose target volumes (CTV1 and GTV) and evaluated dose coverage of the failure site in relation to p16-status in data from a randomized clinical trial [23].

Material and methods

Patients

Patients treated in the randomized phase III trial DAHANCA 19, were eligible for this study [23]. DAHANCA 19 evaluated if adding the EGFR-inhibitor zalutumumab to primary (chemo-)RT would improve outcomes in patients with HNSCC by the intention-to-treat principle. From November 2007 to June 2012, 608 patients from Denmark and Norway with biopsy-proven HNSCC of the oral cavity, oropharynx, hypopharynx and larynx were accrued. Patients were offered primary accelerated RT (predominantly 66–68 Gy, 2 Gy/Fx, 6 Fx/w), daily hypoxic radiosensitization with nimorazole and weekly cisplatin (40 mg/m^2) in case of stage III/IV (IUCC6). Patients were randomized 1:1 to control or intervention with addition of zalutumumab (8 mg/kg weekly during RT). The addition of concomitant zalutumumab showed no effect on the primary endpoint, five-year loco-regional control [23].

The 2004 version of the DAHANCA guidelines were used in the DAHANCA 19 study. During this period GTV-CTV margin recommendations were loosely defined which has been shown to vary between centres from 0 mm to large anatomical margins [13]. Three dose-levels were used with a high-dose CTV1 (66–68 Gy), and a CTV2 (60 Gy) including CTV1 and optionally the first non-involved lymph-node level. CTV3 (50 Gy) included the relevant elective lymph node stations [24].

Patients who completed primary curative RT were included in the current study. Loco-regional failure was defined as both persistent disease (detected within three months post-treatment) or recurrent disease (histological and/or clear radiological evidence of nodal or mucosal tumor after three months) with a cut-off at five years post-treatment. Distant metastasis was defined as a recurrent tumor below the clavicle or above the skull base.

For a register-based pattern of failure analysis, the entire cohort was considered. Failures were registered as tumor (T), nodal (N) or metastatic (M) failures or a combination of these.

Ethics

The Southern Norwegian Research Ethics Committee (S-073774b), The Norwegian Medicines Agency (08/00215-14), The Danish Medicines Agency (2612-3486) and The Central Denmark Region Committees on Health Research Ethics (20070091) granted approval for the DAHANCA 19 study (Clinical Trials: NCT00496652). Subsequently, approval for the collection of planning and diagnostic scans for the current study was obtained.

Point of origin analysis

Point of origin analysis included patients with loco-regional failure, with available failure scan (MRI- or (PET-)CT-scan) conducted upon failure within five years from end-of-therapy. Planning CT-scans (pCTs) with original structure sets and dose plans were uploaded to the national DICOM Collaboration system (DcmCollab) [25,26]. For patients with loco-regional failure, failure scans performed at suspected or verified loco-regional failure (before any treatment intervention) were uploaded to the database. Both pCTs and failure scans were imported to MIM Software (Cleveland, USA, version 7.2) and the volumes of the failure sites were contoured on the failure scans. These were contoured in separate volumes for patients with more than one simultaneous loco-regional failure site (multifocal failure). Failure sites were categorized as either of mucosal or nodal origin per failure site. A head and neck radiation oncologist (MHK) performed the contouring with guidance from the radiologist's description, clinical observation and histopathological reports. Cases were discussed with a head and neck specialist (JGE).

Image co-registrations of failure scans to pCTs were performed in MIM with the failure scan as the primary. Adjustments of the anatomical location of the rigidly fused failure scans could be performed prior to deformable co-registration with the pCT. Deformable image co-registration (DIR) for the MRI-based failure scans was conducted with a multi-modality setting in MIM and with a smoothness factor of 2.0. For CT-based failure scans, the same subject-deformable image registration type was utilized. The method of the PO-analyses is shown in Supplementary Fig. S1 [16].

As previously described, the centre of mass of the failure volume was calculated as the average voxel position evaluated over all voxels within the failure volume [16]. This process reduced the entire failure volume to a single point – the point of origin (PO). The DIR-process enabled the transformation of POs of the failures to the pCTs. In cases where the PO was estimated to be located within air cavities on the pCT (12 failure sites), the PO site was discussed and relocated (JGE + MHK). The POs of the failures were analysed in relation to the original target volumes and dose plan from the pCT.

Spatial analysis

For analyses of the spatial relation between failures and RT target volumes, the distances in three dimensions from the POs to the closest border of target volumes (CTV1 and GTV) were calculated. If the distance between the PO and the border of the target volume was negative, the origin of the failure was estimated to have arisen from within the specific volume, and outside the volume in POs with positive distances.

Dosimetric analysis

To extract the radiation dose to the estimated site of origin of the failures, a sphere with a radius of three mm was created around the POs. This radius corresponds to the uncertainties of DIR of both CT and MRI [27,28]. From the original dose plan of the pCT, absolute minimum and mean doses to the POs were extracted, resulting in estimated coverage of the PO of the failures. Failures were considered covered by curative doses if the mean dose to the sphere around the PO of the failure was $\geq$95 % of the prescribed dose to CTV1 and not covered if $<$95 %.

Tumor tissue analysis

p16-status was evaluated by standard immunohistochemistry

(antibody clone JC8) on primary tumor tissue with a cut-off of 70 % staining in both the nucleus and cytoplasm of the malignant cells. p16 served as a pseudomarker for HPV-driven primary tumors for patients with OPSCC (p16 + OPSCC). Patients with unknown p16 status were considered as being negative.

Statistical analyses

Using descriptive statistics, patient, tumor and treatment characteristics between groups were analysed. Two groups were formed for patients with loco-regional failure: One including patients where the PO analysis was successful, and one where imaging was not performed or was unavailable.

To identify potential clinical or tumor-specific parameters associated with a higher risk of high-dose failure, groups of patients with and without high-dose failure were compared. Mann-Whitney exact tests were applied to continuous variables and Fischer's Exact to categorical variables. P-values < 0.05 were used as an indication of a difference between groups. Hazard ratios for the risk of five-year high-dose failure was estimated using cause-specific univariable Cox-regression. Multivariable analysis was performed for parameters with significance level < 0.05. Analyses were performed in SPSS Statistics (IBM, version 28) and Stata (StataCorp, version 18).

Results

Among the 600 patients who completed curatively intended primary RT, 183 were diagnosed with failure (Fig. 1). The Euler diagram in Fig. 2 shows the failure distribution according to site within the five-year follow-up period. The majority had loco-regional disease upon failure (n = 151). Considering loco-regional failures, one third (51/151) of the patients were diagnosed with failure within the first 3 months post-treatment (persistent disease).

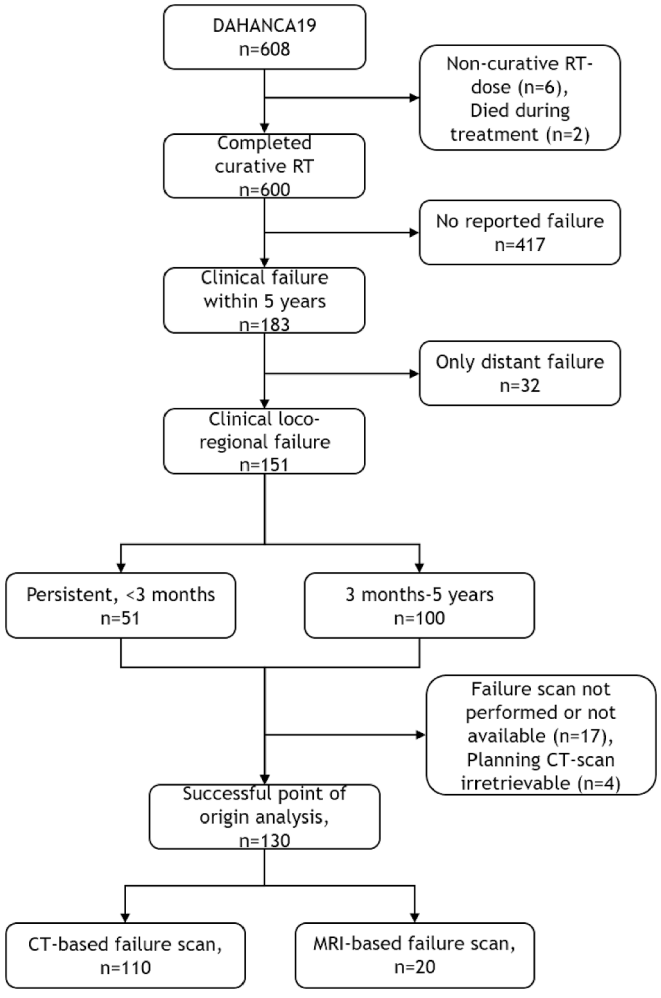

Fig. 1. Flow chart of patients included in the analysis.

Patient characteristics are presented in Table 1.

Pairs of scans (pCT + failure scan) were available for 130 patients, which allowed for PO-analysis. Characteristics and tests for the similarity between the patients with available scans compared to the group of patients without available pCT or failure scan are shown in Supplementary Table T1. No differences between groups were identified.

For the 130 patients where PO-analysis was successful, 189 individual loco-regional failure volumes were contoured (107 nodal and 82 mucosal). The majority of patients (72 %, n = 94) had one site of failure. The number of failure sites for patients with multifocal failure patterns was distributed as two (n = 22), three (n = 8), four (n = 3) and five (n = 3) POs.

Of all failure site POs (both uni- and multifocal failures) where the spatial relationship between the PO and CTV1 was evaluated, 55 % were located within CTV1. Of the patients where the PO-analysis was performed, 87 (67 %) patients had at least one failure site estimated to have originated from within the high-dose target (CTV1). Of 82 T-site failures, 47 (57 %) had a PO within CTV1. This was similar for N-site failures, where 57 (53 %) of 107 nodal POs were located inside CTV1. The relation of POs to target volumes and RT-coverage classification (covered/not covered by 95 % of prescribed high-dose) is depicted in Fig. 3. These stacked bar charts show that high-dose RT covered POs were within 10 mm from CTV1 except in one case (Fig. 3).

The result of the dose-coverage analysis showed that 104 (80 %) of the patients had at least one loco-regional failure site PO that was covered (mean dose to sphere) by at least 95 % of prescribed dose (high-dose failure). Considering all failure site POs, 130 of 189 (69 %) were high-dose failures (Fig. 4). The majority of failures from primary p16 + OPSCC were high-dose failures, as 84 % (16 of 19) of mucosal failure POs and 61 % (30 of 49) of nodal failure POs were covered by at least 95

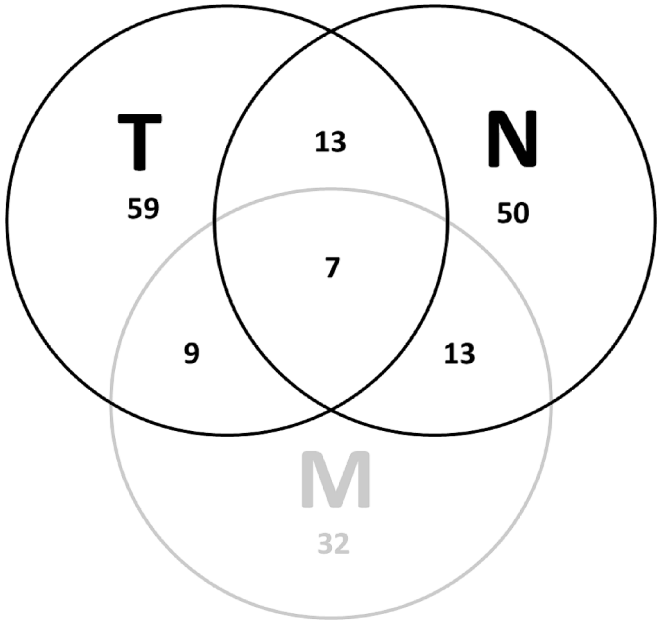

Fig. 2. Euler diagram of pattern of failure from end of RT including 5-year follow-up showing the distribution of clinically reported failure according to site. T: Tumor site, N: Nodal site, M: Distant metastases. For patients with distant metastasis (n = 61), the sites of failure were lung (n = 43), skeletal (n = 22), lymph nodes outside neck (n = 19), liver (n = 10), brain (n = 3), cutaneous (n = 2) and six sites without reported specifications.

Table 1
Patient characteristics for patients with at least one loco-regional high-dose failure compared to patients where no high-dose failure were observed within five years. The no high-dose failure group consist of patients where no loco-regional or distant failure were diagnosed and patients with loco-regional failure where none of the failure sites were high-dose failures or where no scan upon failure were performed. Frequency (percentage) is listed for categorical variables while mean (standard deviation) is displayed for continuous variables. For comparison between groups with and without high-dose failure, Mann-Whitney exact test was used for comparison of continuous variables and Fischer's Exact Test for comparison of categorical variables. Two-sided *p*-values are shown. Hazard ratios were estimated using cause-specific Cox-regression with five-year high-dose failure as the endpoint. The reference variables are listed in the categories (ref).

	All	No high-dose failure	High-dose failure	*p*-value	Hazard ratio (HR [95 % CI])
N	600 (100 %)	496 (83 %)	104 (17 %)		
Age (per year)	58 (8)	59 (8)	57 (8)	0.06	0.98 [0.96–1.00]
Sex					
Male (ref)	492 (82 %)	409 (82 %)	83 (80 %)	0.57	
Female	108 (18 %)	87 (18 %)	21 (20 %)		1.07 [0.66–1.73]
Performance status					
0 (ref)	459 (76 %)	394 (79 %)	65 (62 %)	<0.01	
1–2	141 (24 %)	102 (21 %)	39 (38 %)		2.24 [1.51–3.34]
Pack years					
<30 (ref)	292 (49 %)	253 (51 %)	39 (38 %)	0.01	
≥30	308 (51 %)	243 (49 %)	65 (62 %)		1.72 [1.16–2.56]
Primary tumor					
OPSCC p16+ (ref)	306 (51 %)	270 (54 %)	36 (35 %)	<0.01	
OPSCC p16−	114 (19 %)	87 (18 %)	27 (26 %)		2.31 [1.40–3.80]
Oral cavity	22 (4 %)	15 (3 %)	7 (7 %)		3.11 [1.38–7.00]
Hypopharynx	71 (12 %)	55 (11 %)	16 (15 %)		2.37 [1.32–4.28]
Larynx	87 (14 %)	69 (14 %)	18 (17 %)		1.93 [1.10–3.40]
T-category*					
T1-2 (ref)	364 (61 %)	312 (63 %)	52 (50 %)	0.02	
T3-4	236 (39 %)	184 (37 %)	52 (50 %)		1.75 [1.19–2.57]
N-category*					
N0-1 (ref)	209 (35 %)	179 (36 %)	30 (29 %)	0.18	
N2-3	391 (65 %)	317 (64 %)	74 (71 %)		1.41 [0.92–2.16]
Stage*					
I-II (ref)	297 (50 %)	265 (53 %)	32 (31 %)	<0.01	
III-VI	303 (50 %)	231 (47 %)	72 (69 %)		2.58 [1.70–3.91]
Differentiation grade					
Low/undiff. (ref)	321 (54 %)	272 (55 %)	49 (47 %)	0.16	
Moderate/high	279 (46 %)	224 (45 %)	55 (53 %)		1.35 [0.92–1.10]
Chemotherapy cycles					
0 (ref)	170 (28 %)	141 (28 %)	29 (28 %)	0.97	
1–4	104 (17 %)	87 (18 %)	17 (16 %)		0.94 [0.51–1.70]
5 or more	326 (54 %)	268 (54 %)	58 (56 %)		1.01 [0.64–1.57]
Zalutumumab					
Zalutumumab (ref)	298 (50 %)	246 (50 %)	52 (50 %)	1.00	
Placebo	302 (50 %)	250 (50 %)	52 (50 %)		0.98 [0.67–1.44]

* IUCC TNM-classification converted to 8th edition.

% of prescribed high-dose. For p16− tumors (oral cavity, OPSCC p16-negative, hypopharyngeal or laryngeal), 75 % (47 of 63) of mucosal and 66 % (38 of 58) of nodal failures were high-dose failures. Of 56 POs from persistent failures, 53 were high-dose failures (Supplementary, Fig. S2).

For failures considered not covered by 95 % of prescribed dose to CTV1, the majority of POs were covered by standard elective doses for lymph node stations (50 (CTV3)-60 Gy (CTV2)). For patients with only one failure site (nodal: n = 43 (22 p16 + OPSCC; 21 p16− tumors), mucosal: n = 51 (12 p16 + OPSCC p16+; 39 p16− tumors)), similar patterns were seen (Supplementary, Fig. S3).

Patients with high-dose failure were in poorer performance status (Hazard ratio (HR): 2.24 [95 % confidence interval (CI):1.51–3.34]) and had more pronounced smoking history (HR: 1.72[7.16–2.56]) compared to patients with no high-dose failure (Table 1). Tumor characteristics associated with an increased hazard of high-dose failure were larger T-category (HR: 1.75 [1.19–2.57]), higher stage (HR: 2.58 [1.70–3.91]) and all p16− tumors compared to OPSCC p16 +. In multivariable analysis, higher performance status (WHO1-2) (HR: 1.70 [1.10–2.60]) and clinical stage III-IV (HR: 2.00 [1.15–3.48]) were associated with increased risk of high-dose failure.

Discussion

This is the largest (n = 130) study of PO-based pattern of failure analysis after primary curative intended RT for HNSCC from a randomized trial. Results align with previous studies, confirming that loco-regional failure in HNSCC mainly occurs in the high-dose volume, since 80 % of patients with failure had at least one high-dose failure.

In alignment with Zukauskaite et al., the present study demonstrated that all failure POs, except one, within 10 mm from CTV1 were covered by curative doses [13,16].

In this series, the majority of failures in both p16 + OPSCC and p16− tumors were within or in close proximity to the high-dose regions. A similar pattern was identified by Nissi et al. using volumetric overlap between the PET-positive recurrence volume and the 95 % isodose volume for PTV [10]. Since HPV-driven OPSCC are presumed to be more radiosensitive than non-HPV driven tumors [4,29,30], it might be expected, that most failures in p16 + OPSCC would arise from low-dose areas (geographical misses). However, most failures for p16 + OPSCC in this study were high-dose failures Thus, HPV-driven HNSCC may show a diverse/heterogeneous response to RT in line with Spiotto et al. [29].

Besides radioresistance, failures can be due to geographical misses, i.e., not included in target volumes. The causality behind the not-covered failures in this study is multifactorial. The decision whether to include for instance a slightly enlarged, not-biopsied lymph node in the CTV1 or not resides on a clinical decision. This decision relies on the available clinical data, i.e. pathologic, clinical examinations, radiologic, etc.. Since this study was conducted at a time in Denmark and Norway, where PET-CT in the RT-planning setup was not fully implemented, some of the not-covered nodal failure sites could have had an imaging-detectable disease in the work-up phase of RT-planning. Thereby these sites

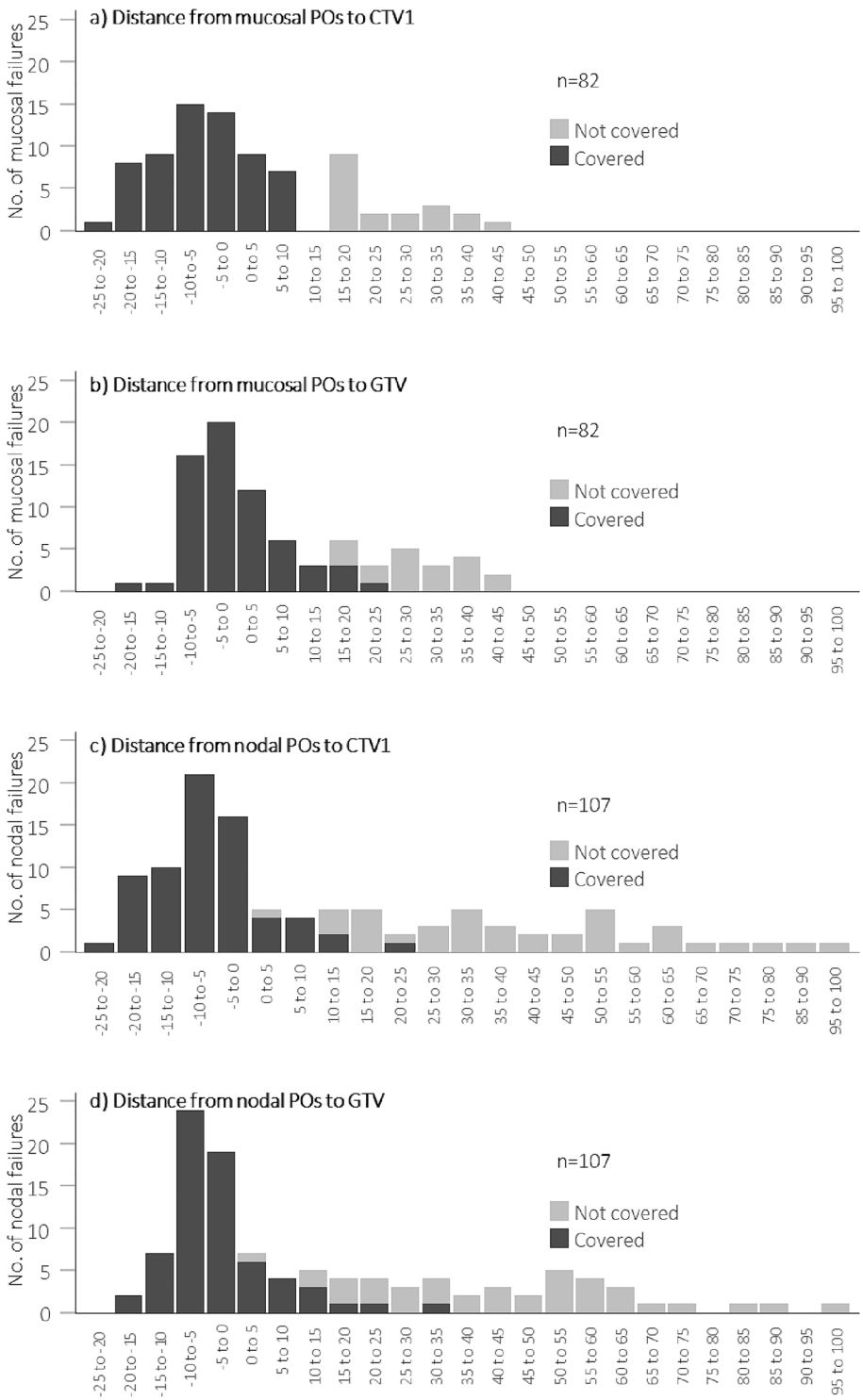

Fig. 3. Histograms of distances from point of origin of failures to GTV and CTV1 for mucosal and nodal failures. Y-axis: number of failures within the category; X-axis: categories based on distance from the point of origin to the closest border of the target volumes in mm.; a) Distances from mucosal failures to CTV1; b) Distances from mucosal failures to GTV; c) Distances from nodal failures to CTV1; d) Distances from nodal failures to GTV. For the one nodal failure in *c* and *d*, within 0–5 mm from GTV and CTV that was not covered, the distance from the PO to CTV1 was 2 mm. The patient had a large GTV-N in close proximity to the skin. The failure was a skin recurrence close to the superficial border of the original GTV-N, where dose was lower.

would have been identified up-front and included in the high-dose target. The GTV to CTV1 margins in this study varied since the guidelines at the time defined the CTV1 rather loosely. Hence, margins varied from no margins (0 mm) to anatomical margins (often > 10 mm). Analysis of the relation between margins and high-dose failures was not performed here, however Zukauskaite et al found no difference in the distribution of local failures for three Danish centres with different GTV-CTV1 margins [13].

Loco-regional control after primary curative RT has been correlated to biomarkers, such as higher density of putative cancer stem cell (CSC) markers [31]. The stem cell model perceives CSCs as a sub-population of the tumor with the ability to differentiate into viable cancer cells [32].

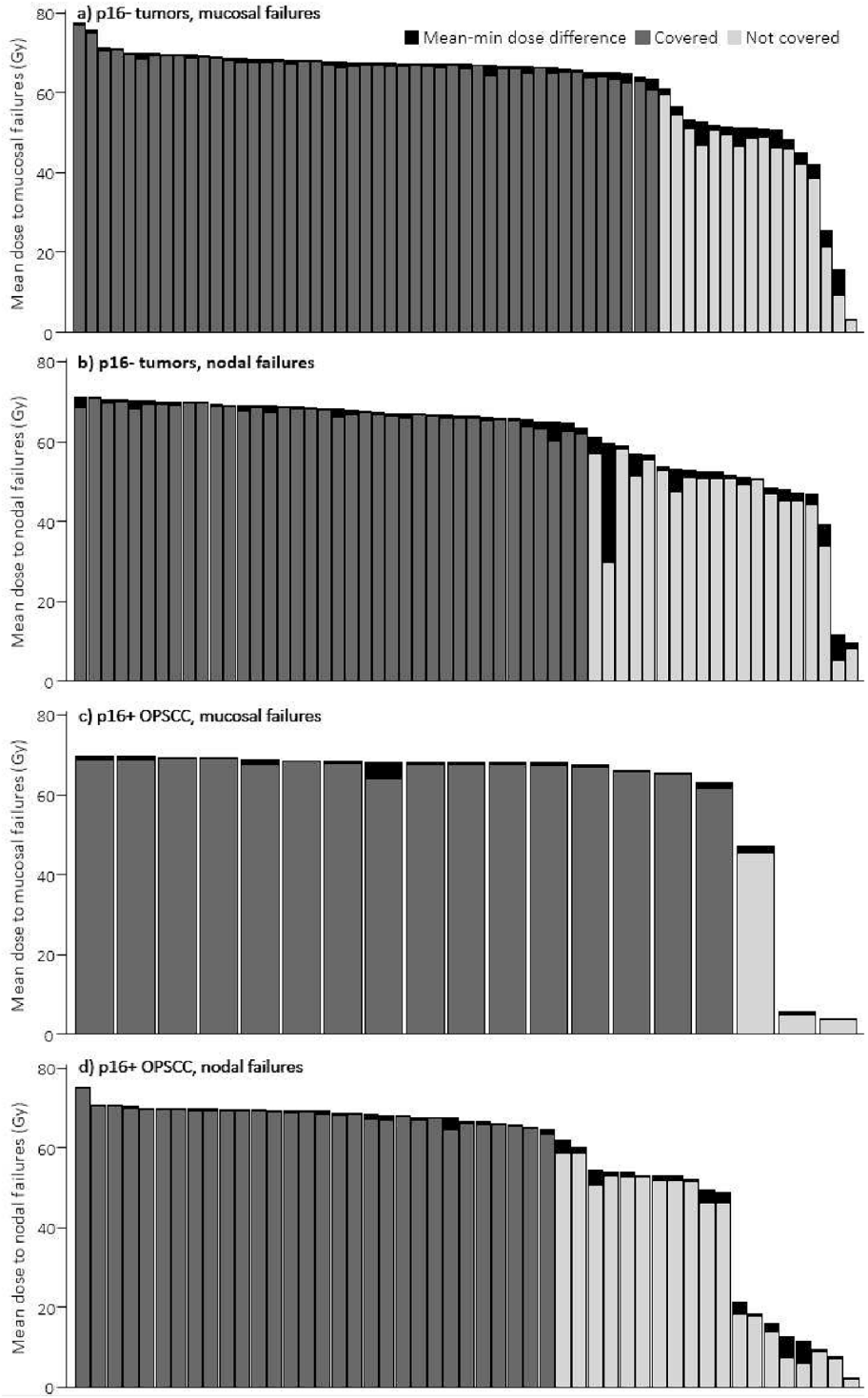

Fig. 4. The entire bar represents mean dose for each point of origin (PO) of the failures. The grey-scaled part of the bars represent minimum dose to the PO and the uppermost black part of the bar represents the difference between mean and minimum dose (mean-min dose difference). The *dark grey bars* are failures with mean dose of at least 95 % of prescribed dose to CTV1. *Light grey bars* are not-covered POs (mean dose to PO < 95 % of prescribed dose). a) is *mucosal* failure POs from primary tumors that were oral cavity, oropharyngeal (OPSCC) p16-negative, hypopharyngeal or laryngeal (p16− tumors); b) is *nodal* failure POs from primary tumors that were p16− tumors; c) is *mucosal* failures where the primary tumor was p16 + OPSCC; d) is *nodal* failures where the primary tumor was p16 + OPSCC. In *b* for one patient (similar to the case in Fig. 3) there was a steep dose gradient within the 6 mm sphere surrounding the PO since it was in close proximity to the skin. This resulted in a dose difference between absolute minimum and mean dose of 30 Gy.

From this model, it is necessary to eliminate all CSCs during the irradiation schedule to achieve tumor control. Applying this model to the concept of treatment failure, the cause of treatment failure could be explained by surviving CSCs [3]. The centre of mass (COM)-approach can be interpreted as an arbitrary approximation of a surviving cancer stem cell from where the failure volume grows spherically. The method may have limitations, as not all tumors grow equally in all directions. However, being less time-dependent as the volumetric approaches; in

time, the recurrence volume will always expand beyond the target volumes, and an originally in-field failure will wrongly be classified as marginal or out-of-field. Chen et al. [21] found that only 40–45 % of recurrences from HPV-positive OPSCC could be classified as volumetrically in-field (>95 % overlap between the recurrent volume and the 95 % isodose). This strict categorization first suggested by Dawson et al. [33] may lead to an underestimation of the proportion of failures with PO within the high-dose target.

The PO-method may not apply to tumors where complete remission was not achieved (persistent disease), since surviving clonogenic tumor cells are more likely distributed throughout the persistent tumor volume. Persistent failures were included in this study to evaluate the assumption, that they were covered by curative doses and thereby presumed caused by radioresistance. Three of 56 persistent failure sites were not covered by curative doses, of which two in retrospect were geographical misses (Supplementary Fig. S2). Since, for the purpose of identifying radioresistant tumors, the best approximation for this endpoint is: Identification of tumor cells that survived the curatively intended RT course, diagnosed after the end of treatment and arising from a site of high RT-dose.

For patients with more than one failure site (multifocal failure), it is not clear whether cancer stem cells survived in all sites of failure or whether the failure arose from one of the sites and later metastasized to the other location(s). However, the similarities between the pattern for all failures (Fig. 4) compared to the pattern for patients with only one failure site (Supplementary Fig. S3) indicate that analysis of all failure sites is representative for the pattern of failure according to dose levels. Therefore, all failure sites were treated equally in the analysis.

In this study, discrimination between recurrent disease and new primaries was based on the clinical evaluation by the trial investigators. This seemed a reasonable approximation, since there exists no general consensus for separation between recurrent disease and new primary tumor. From Fig. 3 it is shown that a few failure volume POs had a distance to the GTV-boarder of up to 4.5 cm. These failures may have represented second primaries or very large failures with a growth pattern extending away from the original tumor site. In retrospect this could not be determined. Therefore, all failure volumes were included and analysed equally to enhance transparency. Future pattern of failure analyses may benefit from the emerging field of DNA-sequencing to discriminate between new primary tumors and recurrent distant metastases [34].

Conclusively, the results of this study suggest radioresistance, rather than geographical misses, as the primary reason for failure following primary radiotherapy for both HPV-positive and negative HNSCC. Hence, dose de-escalation based on HPV/p16 alone might result in inferior treatment outcomes until further radiobiological classification of radiosensitivity has been established. This encourages further research in predictors of the response to RT, where individualization of treatment based on biological features might prove beneficial.

Funding source

Financial support was granted by The Danish National Research Center for Radiotherapy (DCCC-RT) (R191-A11526), The Danish Cancer Society (R231-A13969) and The Health Research Foundation of Central Denmark Region (R64-A3205).

CRediT authorship contribution statement

Morten Horsholt Kristensen: Conceptualization, Methodology, Formal analysis, Investigation, Data curation, Writing – original draft, Visualization, Funding acquisition. **Anne Ivalu Sander Holm:** Methodology, Formal analysis, Investigation, Resources, Writing – review & editing. **Christian Rønn Hansen:** Conceptualization, Methodology, Formal analysis, Resources, Data curation, Writing – review & editing. **Ruta Zukauskaite:** Conceptualization, Methodology, Formal analysis, Resources, Data curation, Writing – review & editing. **Eva Samsøe:** Resources, Data curation, Writing – review & editing. **Christian Maare:** Resources, Data curation, Writing – review & editing. **Jørgen Johansen:** Resources, Data curation, Writing – review & editing. **Hanne Primdahl:** Resources, Data curation, Writing – review & editing. **Åse Bratland:** Resources, Data curation, Writing – review & editing. **Claus Andrup Kristensen:** Resources, Data curation, Writing – review & editing. **Maria Andersen:** Resources, Data curation, Writing – review & editing. **Jens Overgaard:** Conceptualization, Methodology, Resources, Writing – review & editing. **Jesper Grau Eriksen:** Conceptualization, Methodology, Formal analysis, Resources, Data curation, Writing – review & editing, Supervision, Funding acquisition.

Declaration of competing interest

The authors declare that they have no known competing financial interests or personal relationships that could have appeared to influence the work reported in this paper.

Appendix A. Supplementary data

Supplementary data to this article can be found online at https://doi.org/10.1016/j.ctro.2024.100772.

References

[1] Pagh A, Grau C, Overgaard J. Failure pattern and salvage treatment after radical treatment of head and neck cancer. Acta Oncol 2016;55:625–32. https://doi.org/10.3109/0284186X.2015.1117136.
[2] Peitzsch C, Tyutyunnykova A, Pantel K, Dubrovska A. Cancer stem cells: The root of tumor recurrence and metastases. Semin Cancer Biol 2017;44:10–24. https://doi.org/10.1016/j.semcancer.2017.02.011.
[3] Baumann M, Krause M, Hill R. Exploring the role of cancer stem cells in radioresistance. Nat Rev Cancer 2008;8:545–54. https://doi.org/10.1038/nrc2419.
[4] Sørensen BS, Busk M, Olthof N, Speel EJ, Horsman MR, Alsner J, et al. Radiosensitivity and effect of hypoxia in HPV positive head and neck cancer cells. Radiother Oncol 2013;108:500–5. https://doi.org/10.1016/j.radonc.2013.06.011.
[5] Baumann M, Krause M, Overgaard J, Debus J, Bentzen SM, Daartz J, et al. Radiation oncology in the era of precision medicine. Nat Rev Cancer 2016;16:234–49. https://doi.org/10.1038/nrc.2016.18.
[6] Lassen P, Primdahl H, Johansen J, Kristensen CA, Andersen E, Andersen LJ, et al. Impact of HPV-associated p16-expression on radiotherapy outcome in advanced oropharynx and non-oropharynx cancer. Radiother Oncol 2014;113:310–6. https://doi.org/10.1016/j.radonc.2014.11.032.
[7] Tandon S, Gairola M, Ahlawat P, Karimi AM, Tiwari S, Muttagi V, et al. Failure patterns of head and neck squamous cell carcinoma treated with radical radiotherapy by intensity modulated radiotherapy technique using focal volume and dosimetric method. Head Neck 2019;41:1632–7. https://doi.org/10.1002/hed.25586.
[8] Burr AR, Harari PM, Ko HC, Bruce JY, Kimple RJ, Witek ME. Reducing radiotherapy target volume expansion for patients with HPV-associated oropharyngeal cancer. Oral Oncol 2019;92:52–6. https://doi.org/10.1016/j.oraloncology.2019.03.013.
[9] Raktoe SAS, Dehnad H, Raaijmakers CPJ, Braunius W, Terhaard CHJ. Origin of tumor recurrence after intensity modulated radiation therapy for oropharyngeal squamous cell carcinoma. Int J Radiat Oncol Biol Phys 2013;85:136–41. https://doi.org/10.1016/j.ijrobp.2012.02.042.
[10] Nissi L, Suilamo S, Kytö E, Vaittinen S, Irjala H, Minn H. Recurrence of head and neck squamous cell carcinoma in relation to high-risk treatment volume. Clin Transl Radiat Oncol 2021;27:139–46. https://doi.org/10.1016/j.ctro.2021.01.013.
[11] Ferreira BC, Marques RV, Khouri L, Santos T, Sá-Couto P, Lopes MDC. Assessment and topographic characterization of locoregional recurrences in head and neck tumours. Radiat Oncol 2015;10:41. https://doi.org/10.1186/s13014-015-0345-4.
[12] Almarzouki H, Niazi T, Hier M, Mlynarek A, Lavoie I, Sultanem K. Local failure rate in oropharyngeal carcinoma patients treated with intensity-modulated radiotherapy without high-dose clinical target volume. Cureus 2018;10. https://doi.org/10.7759/cureus.2958.
[13] Zukauskaite R, Hansen CR, Grau C, Samsøe E, Johansen J, Petersen JBB, et al. Local recurrences after curative IMRT for HNSCC: Effect of different GTV to high-dose CTV margins. Radiother Oncol 2018;126:48–55. https://doi.org/10.1016/j.radonc.2017.11.024.
[14] de Ridder M, Gouw ZAR, Sonke JJ, Navran A, Jasperse B, Heukelom J, et al. Recurrent oropharyngeal cancer after organ preserving treatment: pattern of failure and survival. Eur Arch Oto-Rhino-Laryngol 2017;274:1691–700. https://doi.org/10.1007/s00405-016-4413-7.
[15] Mohamed ASR, Wong AJ, Fuller CD, Kamal M, Gunn GB, Phan J, et al. Patterns of locoregional failure following post-operative intensity-modulated radiotherapy to

oral cavity cancer: quantitative spatial and dosimetric analysis using a deformable image registration workflow. Radiat Oncol 2017;12:1–12. https://doi.org/10.1186/s13014-017-0868-y.

[16] Zukauskaite R, Hansen CR, Brink C, Johansen J, Asmussen JT, Grau C, et al. Analysis of CT-verified loco-regional recurrences after definitive IMRT for HNSCC using site of origin estimation methods. Acta Oncol 2017;56:1554–61. https://doi.org/10.1080/0284186X.2017.1346384.

[17] De Felice F, Thomas C, Barrington S, Pathmanathan A, Lei M, Urbano TG. Analysis of loco-regional failures in head and neck cancer after radical radiation therapy. Oral Oncol 2015;51:1051–5. https://doi.org/10.1016/j.oraloncology.2015.08.004.

[18] Bayman E, Prestwich RJD, Speight R, Aspin L, Garratt L, Wilson S, et al. Patterns of failure after intensity-modulated radiotherapy in head and neck squamous cell carcinoma using compartmental clinical target volume delineation. Clin Oncol 2014;26:636–42. https://doi.org/10.1016/j.clon.2014.05.001.

[19] Due AK, Vogelius IR, Aznar MC, Bentzen SM, Berthelsen AK, Korreman SS, et al. Recurrences after intensity modulated radiotherapy for head and neck squamous cell carcinoma more likely to originate from regions with high baseline [18F]-FDG uptake. Radiother Oncol 2014;111:360–5. https://doi.org/10.1016/j.radonc.2014.06.001.

[20] Mohamed ASR, Cardenas CE, Garden AS, Awan MJ, Rock CD, Westergaard SA, et al. Patterns-of-failure guided biological target volume definition for head and neck cancer patients: FDG-PET and dosimetric analysis of dose escalation candidate subregions. Radiother Oncol 2017;124:248–55. https://doi.org/10.1016/j.radonc.2017.07.017.

[21] Chen AM, Chin R, Beron P, Yoshizaki T, Mikaeilian AG, Cao M. Inadequate target volume delineation and local–regional recurrence after intensity-modulated radiotherapy for human papillomavirus-positive oropharynx cancer: Local–regional recurrence after IMRT for HPV-positive oropharynx cancer. Radiother Oncol 2017;123:412–8. https://doi.org/10.1016/j.radonc.2017.04.015.

[22] Leeman JE, Li Jg, Pei X, Venigalla P, Zumsteg ZS, Katsoulakis E, et al. Patterns of treatment failure and postrecurrence outcomes among patients with locally advanced head and neck squamous cell carcinoma after chemoradiotherapy using modern radiation techniques. JAMA Oncol 2017;3:1487–94. https://doi.org/10.1001/jamaoncol.2017.0973.

[23] Eriksen JG, Maare C, Johansen J, Primdahl H, Evensen JF, Kristensen CA, et al. Evaluation of the EGFR-inhibitor zalutumumab given with primary curative (chemo)radiation therapy to patients with squamous cell carcinoma of the head and neck: results of the DAHANCA 19 randomized phase 3 trial. Int J Radiat Oncol 2014;88:465. https://doi.org/10.1016/j.ijrobp.2013.11.021.

[24] Grégoire V, Levendag P, Ang KK, Bernier J, Braaksma M, Budach V, et al. CT-based delineation of lymph node levels and related CTVs in the node-negative neck: DAHANCA, EORTC, GORTEC, NCIC, RTOG consensus guidelines. Radiother Oncol 2003;69:227–36. https://doi.org/10.1016/j.radonc.2003.09.011.

[25] Brink C, Lorenzen EL, Krogh SL, Westberg J, Berg M, Jensen I, et al. DBCG hypo trial validation of radiotherapy parameters from a national data bank versus manual reporting. Acta Oncol 2018;57:107–12. https://doi.org/10.1080/0284186X.2017.1406140.

[26] Westberg J, Krogh S, Brink C, Vogelius IR. A DICOM based radiotherapy plan database for research collaboration and reporting. J Phys Conf Ser 2014;489:1–5. https://doi.org/10.1088/1742-6596/489/1/012100.

[27] Zukauskaite R, Brink C, Hansen CR, Bertelsen A, Johansen J, Grau C, et al. Open source deformable image registration system for treatment planning and recurrence CT scans: validation in the head and neck region. Strahlenther Onkol 2016;192:545–51. https://doi.org/10.1007/s00066-016-0998-4.

[28] Kristensen MH, Hansen CR, Zukauskaite R, Johansen J, Samsøe E, Maare C, et al. Co-registration of radiotherapy planning and recurrence scans with different imaging modalities in head and neck cancer. Phys Imaging Radiat Oncol 2022;23:80–4. https://doi.org/10.1016/j.phro.2022.06.012.

[29] Spiotto MT, Taniguchi CM, Klopp AH, Colbert LE, Lin SH, Wang L, et al. Biology of the radio- and chemo-responsiveness in HPV malignancies. Semin Radiat Oncol 2021;31:274–85. https://doi.org/10.1016/j.semradonc.2021.02.009.

[30] Rieckmann T, Tribius S, Grob TJ, Meyer F, Busch CJ, Petersen C, et al. HNSCC cell lines positive for HPV and p16 possess higher cellular radiosensitivity due to an impaired DSB repair capacity. Radiother Oncol 2013;107:242–6. https://doi.org/10.1016/j.radonc.2013.03.013.

[31] Linge A, Schmidt S, Lohaus F, Krenn C, Bandurska-Luque A, Platzek I, et al. Independent validation of tumour volume, cancer stem cell markers and hypoxia-associated gene expressions for HNSCC after primary radiochemotherapy. Clin Transl Radiat Oncol 2019;16:40–7. https://doi.org/10.1016/j.ctro.2019.03.002.

[32] Baumann M, Krause M, Thames H, Trott K, Zips D. Cancer stem cells and radiotherapy. Int J Radiat Biol 2009;85:391–402. https://doi.org/10.1080/09553000902836404.

[33] Dawson LA, Anzai Y, Marsh L, Martel MK, Paulino A, Ship JA, et al. Patterns of local-regional recurrence following parotid-sparing conformal and segmental intensity-modulated radiotherapy for head and neck cancer. Int J Radiat Oncol Biol Phys 2000;46:1117–26. https://doi.org/10.1016/S0360-3016(99)00550-7.

[34] Lilja-Fischer JK, Saksø M, Stougaard M, Steiniche T, Overgaard J. Distinguishing recurrence and new primary tumor as well as the origin of neck metastases in head and neck cancer clinical trials by targeted DNA sequencing. Acta Oncol 2019;58:1506–8. https://doi.org/10.1080/0284186X.2019.1629015.